Astronomy & Astrophysics

Where does the hard X-ray diffuse emission in clusters of galaxies come from?

S. Colafrancesco[1], P. Marchegiani[2], and G. C. Perola[1,2]

[1] INAF - Osservatorio Astronomico di Roma, via Frascati 33, 00040 Monteporzio, Italy
    e-mail: cola@mporzio.astro.it
[2] Dipartimento di Fisica, Università Roma 3, via della Vasca Navale 84, Roma, Italy

ABSTRACT

The surface brightness produced by synchrotron radiation in clusters of galaxies with a radio-halo sets a degenerate constraint on the magnetic field strength, the relativistic electron density and their spatial distributions, $B(r)$ and $n_{rel}(r)$, in the intracluster medium. Using the radio-halo in the Coma Cluster as a case study, with the radio brightness profile and the spectral index as the only constraints, predictions are made for the brightness profiles expected in the 20–80 keV band due to Inverse Compton Scattering (ICS) by the relativistic electrons on the Cosmic Microwave Background. This is done for a range of central values of the magnetic field, B, and models of its radial dependence, $B(r)$ (of which two represent extreme situations, namely a constant value either of B or of $n_{rel}(r)$, the third a more realistic intermediate case). It is shown that the possible presence of scalar fluctuations on small scales in the strength of B tends to systematically depress the electron density required by the radio data, hence to decrease the ICS brightness expected. These predictions should be useful to evaluate the sensitivity required in future imaging HXR instruments, in order to obtain direct information on the spatial distribution and content of relativistic electrons, hence on the magnetic field properties. If compared with the flux in the HXR tail, whose detection has been claimed in the Coma cluster (Fusco-Femiano et al. 2004, ApJ, 602, L73), when interpreted as ICS from within the radius R_h of the radio-halo, as measured so far, the predictions lead to central values B_0 that are significantly lower than those which have been obtained (albeit still controversial) from Faraday Rotation measurements. The discrepancy is somewhat reduced if the radio-halo profile is hypothetically extrapolated out to R_{vir}, that is about three times R_h, or, as suggested by hydrodynamical simulations (Dolag et al. 2002, A&A, 387, 383), if it is assumed that $B(r) \propto n_{th}(r)$. In the latter case $n_{rel}(r)$ has its minimum value at the center of the cluster. If real and from ICS, the bulk of the HXR tail should then be contributed by electrons other than those responsible for the bulk of the radio-halo emission. This case illustrates the need for spatially resolved spectroscopy in the HXR, in order to obtain solid information on the non-thermal content of clusters of galaxies.

Key words. cosmology: theory – galaxies: clusters: general – cosmology: diffuse radiation – radiation mechanisms: non-thermal

1. Introduction

Radio halos in galaxy clusters are extended sources with a low surface brightness permeating the central cluster regions. They show an approximately regular shape, resembling the cluster X-ray halo, a steep radio spectrum $J_\nu \propto \nu^{-\alpha_R}$ with spectral index α_R typically $\gtrsim 1$, and little or no polarization (see, e.g., Feretti 2003 for an observational review). Cluster radio halos are generally quite extended with radii $R_h \gtrsim 1$ Mpc, even though smaller halos (with $R_h \lesssim 0.5$ Mpc radii) have also been detected. The one in the Coma cluster, which is usually considered the archetype of this population of radio sources, has $R_h \approx 0.9 \, h_{70}^{-1}$ Mpc.

The spectral slopes fall in the range $0.7 \lesssim \alpha_R \lesssim 2$ (as obtained from WENSS and NVSS observations at 327 and 1400 GHz, respectively; see, e.g., the data compilation in Kempner & Sarazin 2001). In a few well-studied cases, with a wider frequency coverage, the spectral shape is known with

better accuracy. In particular, the Coma radio-halo spectrum has been studied from ~30 MHz to ~5 GHz, and can be fitted by a single power-law with $\alpha_R \approx 1.35$ in the frequency range 30−1400 MHz (Deiss et al. 1997). More recent data indicate a steepening at $\nu > 1.4$ GHz (Thierbach et al. 2003). Some evidence has been also reported (Giovannini et al. 1993) that the spectral index α_R between $\nu = 326$ MHz and 1.4 GHz changes from ≈ 0.8 at an angular distance $\theta \approx 3$ arcmin from the Coma cluster center up to ≈ 1.4 at $\theta \approx 12$ arcmin. In this respect, however, Deiss et al. (1997) pointed out that the emission at 1.4 GHz is much more extended than found by Giovannini et al. (1993), thus indicating that the radial increase of α_R might be in fact weaker than claimed.

The widely accepted view is that the radio halos (see, e.g., Brunetti 2003, for a theoretical review) are produced by synchrotron emission from a population of relativistic electrons with energies $E_e \approx 7.9 B_\mu^{-1/2} (\nu/\text{GHz})^{1/2}$ GeV diffusing in the intra-cluster magnetic field B. The electron energy

must be $E_e \gtrsim 1.37 B_\mu^{-1/2}$ GeV in order to emit at frequencies $\nu \gtrsim 30$ MHz. Here B_μ is the value of the intra-cluster magnetic field in the synchrotron emission formulae (see, e.g., Longair 1994), given in μG units.

The radio flux due to a population of relativistic electrons, whose radial density distribution $\eta(r)$ and energy spectrum is given by

$$n_{\mathrm{rel}}(E, r) = n_{\mathrm{rel},0} E^{-x} \eta(r) \tag{1}$$

can be written as

$$F_{\nu,S} \propto n_{\mathrm{rel},0} \nu^{-\alpha_R} \int \mathrm{d}r r^2 \eta(r) [B_\perp(r)]^{\alpha_R+1}, \tag{2}$$

with $\alpha_R = (x - 1)/2$. It clearly depends, in a degenerate way, on the combination of two quantities: the spectrum and the spatial distribution of the relativistic electron density, $n_{\mathrm{rel}}(E, r)$, and the strength and structure of the transverse magnetic field $B_\perp(r)$. In order to resolve this degeneracy, an independent estimate of one of the two quantities is needed.

As noted long ago (Perola & Reinhardt 1972; Harris & Grindlay 1979; Rephaeli 1979), a direct probe would consist of measuring the emission inevitably produced by the Inverse Compton Scattering (ICS) of the same relativistic electrons on the Cosmic Microwave Background (CMB) photons. In particular, relativistic electrons with energies $E_e \gtrsim$ a few GeV would scatter the CMB photons up to the X-ray and gamma-ray energy range. The ICS, on the CMB photons, due to the synchrotron emitting electrons inevitably produces a power-law emission spectrum

$$F_{E,\mathrm{ICS}} \propto n_{\mathrm{rel},0} E^{-\alpha_x} \int \mathrm{d}r r^2 \eta(r) \tag{3}$$

with $\alpha_x \equiv \alpha_R$. Thus a measure of this quantity would yield the number of electrons involved.

By using the Coma cluster as a case-study, the goal of this paper is to predict the brightness distribution of the ICS in the Hard X-Rays (HXR, specifically in the band 20–80 keV) for different choices of the radial dependence, on large scale, of the magnetic field, $B(r)$, using as the only constraint the available information on the (azimuthally averaged) radio brightness distribution. Such predictions are not based on the theoretical issues concerning the origin of non-thermal phenomena in galaxy clusters (for a review of this topic see, e.g., Brunetti 2003), hence in this respect can be considered as model-independent. Our predictions might be useful to assess the potential of HXR imaging devices in this field. In this context, the consequences on the ICS emission related to the small scale structure of the magnetic field (both in direction and strength) will be emphasized.

For the small scale structures of the magnetic field just mentioned, the information available on its longitudinal strength, as obtained (and been inferred already) from Faraday Rotation (FR) measurements, will be used to make our "best" prediction of the spatially integrated ICS HXR emission. This will then be compared with observational results, which claim that this component has been already detected (Fusco-Femiano et al. 1999, 2004; Rephaeli et al. 1999).

The plan of the paper is the following. In Sect. 2 the radio brightness profile of Coma is used to constrain, in a parametric form, the radial dependence of the relativistic electron density and that of the magnetic field, and the relationships between the two. Section 3 is devoted to the impact of both scalar and vectorial fluctuations in the magnetic field on the synchrotron emissivity. In Sect. 4 the relativistic electron density as a function of radius is derived for a set of representative values of the central magnetic field, B_0, and three different radial profiles for $B(r)$. Correspondingly, in Sect. 5 the predicted ICS brightness profiles are illustrated. In Sect. 6 the results are compared with the measurement of a HXR candidate ICS spectral tail in Coma, and discussed also in the light of the available information on the strength of B from Faraday Rotation measurements. Section 7 contains the summary and conclusions. We use $H_0 = 70$ km s^{-1} Mpc^{-1} and a flat, vacuum-dominated cosmology ($\Omega_\Lambda = 0.7, \Omega_m = 0.3$) throughout the paper.

2. The radio-halo surface brightness in Coma

We derive here the constraints on the spatial structure of the magnetic field $B(r)$ and of the relativistic electrons density, $n_{\mathrm{rel}}(E, r)$, in the Coma cluster from the analysis of its radio-halo surface brightness. Since the radio halo emission depends on both the magnetic field amplitude and the relativistic electron density in a degenerate way (see Eq. (2)), the magnetic field spatial structure will be inferred from the radio halo surface brightness observations by assuming parametric models for the spatial distribution of the relativistic electrons.

First, we fit the azimuthally averaged radio brightness profile of Coma observed at $\nu = 1.4$ GHz (Deiss et al. 1997) initially assuming the profile

$$S_\nu(\theta) = S_{\nu,0}\left[1 + \left(\frac{\theta}{\theta_c}\right)^2\right]^{-q'_R} \tag{4}$$

and using the same core radius that fits the cluster X-ray brightness, with $\theta_c = 10.5'$ (Briel et al. 1992). In this case, we find a best fit parameter $q'_R = 1.63 \pm 0.09$ with a reduced χ^2, $\chi^2_{\mathrm{red}} = 2.13$ with 6 d.o.f. (we give hereafter 1σ uncertainties).

Because this fit is not sufficiently accurate, as can be judged in Fig. 1, it was repeated with both q'_R and $\theta_{c,R}$ as free parameters. A much better fit is obtained ($\chi^2_{\mathrm{red}} = 0.40$ with 5 d.o.f., see Fig. 1), with $q'_R = 3.9 \pm 1.2$ and $\theta_{c,R} = 23.8 \pm 6.2$ arcmin. In the following, the parameter values from the second fit will be used.

By adopting these values, along with a value of the spectral index independent from θ, we are implicitly assuming that they apply also to the emission at frequencies lower than $\nu = 1.4$ GHz. At this frequency the electron energy is related to the field strength as $E_e \approx 9.35 B_\mu^{-1/2}$ GeV. Electrons with this energy emit via ICS photons with energy $E_X \sim 700 B_\mu^{-1}$ keV. Therefore, for $B < 8.75 \mu$G, the 20–80 keV ICS emission is due to electrons that emit in radio at frequencies $\nu \lesssim (350-1400)$ MHz. Since we confine ourselves to B values smaller than the limit above, the spectral steepening observed at $\nu > 1400$ MHz (Thierbach et al. 2003) has no effect on our predictions.
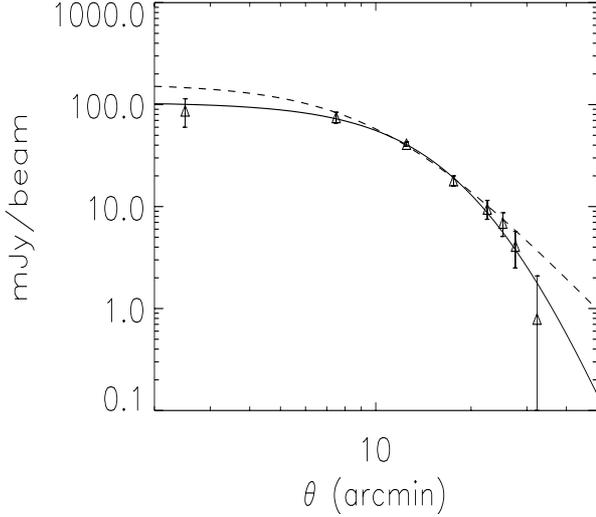
Fig. 1. The spatial distribution of the radio-halo brightness of the Coma cluster fitted with the functional form in Eq. (4): the dashed curve represents the fit with θ_c fixed at 10.5 arcmin from the X-ray profile, the solid curve with the best fit value of $\theta_{c,R} = 23.8$ arcmin. Data are from Deiss et al. (1997).
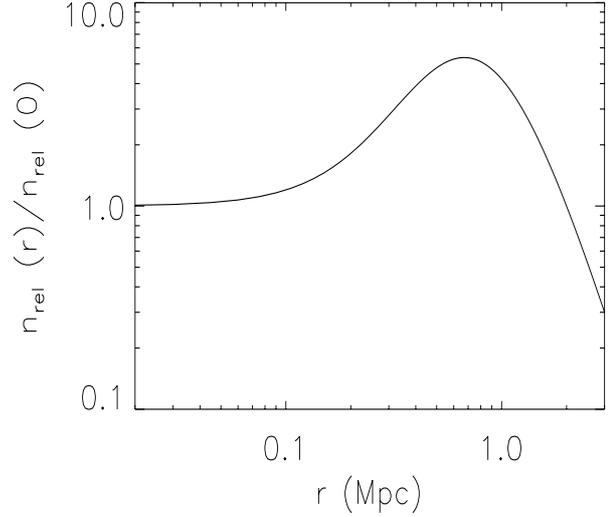

Fig. 2. The radial distribution of the relativistic electrons, if $B(r)$ is assumed to increase with the density of the thermal intracluster gas, as from hydrodynamical simulations by Dolag et al. (2002).

On the other hand, in order to emit via ICS in the 20–80 keV band, the electrons must have energies $E_e \approx 0.35$ GeV$(E/\text{keV})^{1/2} \approx 1.6$–$3.2$ GeV. The radio frequency at which these electrons emit via synchrotron is in the range $\nu \approx (40-60)B_\mu$ MHz. For a value of B as small as $B = 0.2\,\mu$G, their radio emission would fall in the range ≈ 8–32 MHz, which lies completely outside the frequency span of the observations available (see, e.g., Deiss et al. 1997). Therefore, any ICS prediction for values of B_μ less than unity relies, to an extent which increases when B decreases, upon a simple extrapolation of the observed spectrum.

The radial dependence of the synchrotron emissivity, which corresponds to the brightness profile assuming spherical symmetry, is given by

$$J(r) \propto [1 + (r/r_{c,R})^2]^{-q_R} \tag{5}$$

with best-fit parameters $q_R = q'_R + 1/2 = 4.4$ and $r_{c,R} = 0.67\,h_{70}^{-1}$ Mpc.

To convert this dependence into constraints on $B(r)$ and $n_{rel}(r)$, we adopt a simple functional form, namely $n_{rel}(E, r) = n_{rel,0}E^{-x}\eta(r)$ (as in Eq. (1)) $B(r) = B_0 g(r)$, where

$$\eta(r) = [1 + (r/r_{c,R})^2]^{-q_e} \tag{6}$$

$$g(r) = [1 + (r/r_{c,R})^2]^{-q_B}, \tag{7}$$

with the same core radius $r_{c,R}$. It follows that

$$J(r) \propto \eta(r)g(r)^{\beta_R} \tag{8}$$

with $\beta_R = \alpha_R + 1 = 2.35$ (with the adopted value $\alpha_R = 1.35$). In order to reproduce the observed brightness profile, the following relationship must be obeyed:

$$q_e + \beta_R q_B = q_R. \tag{9}$$

We consider, for illustration of the HXR brightness profile to be expected, three cases: i) a uniform distribution of the relativistic electrons, $q_e = 0$, with the corresponding slope $q_B = q_R/\beta_R = 1.87$; ii) the case of a constant pressure ratio between the magnetic field and relativistic electrons, $q_e = 2q_B$, hence $q_B = 1.01$ and $q_e = 2.02$; iii) a uniform magnetic field, $q_B = 0$, with the corresponding slope $q_e = 4.4$.

The first and the last should be regarded as limiting cases. According to hydrodynamical simulations (see, e.g., Gonçalves & Friaça 1999; Dolag et al. 2001, 2002) the magnetic field strength is likely to decrease radially. These simulations indicate, in addition, that the B field fluctuates over a wide range of scales. These fluctuations can be very relevant when it comes to inferring the number of radio-emitting electrons, hence of their ICS emission (see Sect. 3).

A result from hydrodynamical simulations, which seems to be partly supported by observational results on Faraday Rotation (Dolag et al. 2002) – namely that $B(r)$ begaves approximately like the density of the thermal gas – if assumed to hold for Coma, implies what is shown in Fig. 2: that the density of the relativistic electrons, in order to reproduce the radio brightness profile, would have to increase from the center outward up to a maximum at about $0.8R_h$. We regard this as rather unlikely and it seems, to our knowledge, to have been disregarded so far. We shall however return to this situation in Sect. 6.

3. The role of magnetic field structure: radial profile and fluctuations

The intra-cluster magnetic field is likely to consist of a smooth component on top of which there are scalar (amplitude) and vectorial (directional) fluctuations.

Because the synchrotron emissivity depends non-linearly on the amplitude of the transverse component $B_\perp$ of the magnetic field, $J_\nu \propto B_\perp^{\alpha_R+1}$, a radial dependence in the smooth component of B, as well as the fluctuations, do have an impact on

the number of relativistic electrons responsible for the same radio-halo flux.

Concerning the smooth component with profile $B(r) = B_0 g(r)$, one can introduce its volume-averaged value:

$$\langle B \rangle = \frac{\int dV B(r)}{\int dV} = 3 B_0 \left(\frac{r_{c,R}}{R}\right)^3 I, \tag{10}$$

where $I = \int_0^p dx x^2 g(x)$, $x \equiv (r/r_{c,R})$ in terms of the typical core radius $r_{c,R}$ of the magnetic field, and of the maximum radial extension of the magnetic field $R = p r_{c,R}$. For the same volume-averaged value of the magnetic field, we have verified that the volume integrated number of relativistic electrons is larger when $q_B = 0$ than for any other value in the interval $0-1.87$ selected in the previous section.

To obtain a quantitative estimate of the impact of scalar fluctuations, we adopt a simple treatment. Let us assume that, on scales smaller than $l(r)$

$$l(r) \ll \frac{dr}{dB} B(r) \tag{11}$$

where B can be considered independent of r, the strength is subject to fluctuations δB, such that

$$\langle B + \delta B \rangle = B. \tag{12}$$

Hence within $l(r)$

$$\left\langle (B + \delta B)^2 \right\rangle = B^2 + \left\langle (\delta B)^2 \right\rangle. \tag{13}$$

Upon substitution of Eq. (13) in the synchrotron formula, one obtains

$$J(r) \propto n_{\rm rel}(r) B(r)^{\alpha_R + 1} \left[1 + \frac{\langle (\delta B)^2 \rangle}{B^2} \right]^{(\alpha_R + 1)/2}. \tag{14}$$

The factor containing the second order effect of the fluctuations in Eq. (14) is always ≥ 1, and can itself be a function of r. If we assume, for simplicity, that it is independent of r, then one can compute the factor, after integrating over the volume to obtain the flux F_ν, by which the quantity $n_{0,\rm rel}$ is overestimated with respect to the case of zero fluctuations. For example, with the value of α_R adopted for Coma, this factor is equal to 1.12, 1.6, 2.26 for $\langle (\delta B)^2 \rangle / B^2 = 0.1, 0.5$ and 1, respectively.

Vectorial fluctuations are of great importance in the interpretation of Faraday Rotation measurements, yielding

$$RM = \int n_{\rm th} \mathbf{B} \cdot d\boldsymbol{\ell} \tag{15}$$

where $n_{\rm th}$ is the density of thermal electrons inferred from X-ray observations.

These measurements, given the independent constraint on $n_{\rm th}$, are in principle a very good tool to estimate the strength of the B field parallel to the line of sight, along with the coherence scale of the field direction. We shall return to this issue in Sect. 6. Here we recall that the average value of this scale is very much smaller than the cluster radius. To quantify the effects of the directional fluctuations on the emissivity, we assume a random and isotropic distribution. The emissivity formula will therefore contain the term

$$\langle B_\perp^{\alpha_R + 1} \rangle = f(\alpha_R) B^{\alpha_R + 1} = 0.5 \left(\int_0^\pi (\sin\theta)^{2 + \alpha_R} d\theta \right) B^{\alpha_R + 1}. \tag{16}$$

Table 1. The list of parameters used for the calculation of the Coma HXR brightness.

q_e	q_b	B_0 (μG)	$\langle B \rangle$ (μG)	$n_{\rm rel,0}$ (cm^{-3} GeV^{-1})
0	1.87	0.1	0.03	6.46×10^{-10}
2.02	1.01	0.1	0.051	6.46×10^{-10}
4.4	0	0.1	0.1	6.46×10^{-10}
0	1.87	0.2	0.06	1.26×10^{-10}
2.02	1.01	0.2	0.1	1.26×10^{-10}
4.4	0	0.2	0.2	1.26×10^{-10}
0	1.87	0.5	0.15	1.48×10^{-11}
2.02	1.01	0.5	0.255	1.48×10^{-11}
4.4	0	0.5	0.5	1.48×10^{-11}
0	1.87	1	0.3	2.89×10^{-12}
2.02	1.01	1	0.51	2.89×10^{-12}
4.4	0	1	1	2.89×10^{-12}
0	1.87	3	0.9	2.19×10^{-13}
2.02	1.01	3	1.5	2.19×10^{-13}
4.4	0	3	3	2.19×10^{-13}
0	1.87	5	1.5	6.58×10^{-14}
2.02	1.01	5	2.55	6.58×10^{-14}
4.4	0	5	5	6.58×10^{-14}

4. Constraints on the relativistic electron density

If we use the smooth radial distribution of the intra-cluster magnetic field as given by Eq. (7), the normalization of the relativistic electron distribution in Eq. (1) which reproduces the radio-halo flux at 1.4 GHz, $J_{1.4} = 0.64$ Jy (Deiss et al. 1997) can be written as

$$n_{\rm rel,0} = K_{\alpha_R} I_R^{-1} f^{-1}(\alpha_R) \left(\frac{B_0}{\mu G}\right)^{-(\alpha_R + 1)} \quad {\rm cm}^{-3}\,{\rm GeV}^{-1} \tag{17}$$

where $I_R = \int_0^1 dx x^2 [1 + (R_h/r_{c,R})^2 x^2]^{-q_R}$, $f^{-1}(\alpha_R)$ is given by Eq. (16), and $q_R = q_e + \beta_R q_B$. For the choice $\alpha_R = 1.35$, the normalization factor $K \cdot f^{-1}$ in Eq. (17) is equal to 8.64×10^{-14}.

For the predictive purposes declared in Sect. 1, we have adopted the following values of the central magnetic field strength, $B_0 = 0.1, 0.2, 0.5, 1, 3, 5$ μG. For the three combinations of q_e and q_B anticipated in Sect. 2, and $\alpha_R = 1.35$, the quantity $n_{\rm rel,0}$ is given in Table 1, Col. 5, along with, in Col. 4, the volume average of B calculated according to Eq. (10) *within the observed value R_h of the radio-halo*.

For all the combinations of the selected values of B_0, q_e and q_B, we show in Figs. 3–5, as a function of the radial distance from the center, the pressures contributed by the relativistic electrons, $P_{\rm rel}$, by the magnetic field, P_B and by the thermal gas, $P_{\rm thermal}$. The relativistic electron pressure was evaluated assuming $E_{\rm min} = 1$ GeV. The pressure profiles in these figures are extrapolated out to $R_{\rm vir}$, which is approximately equal to 3 Mpc (Lokas & Mamon 2003).

The pressure of the relativistic electrons needed to fit the radio-halo brightness of Coma strongly decreases with increasing values of the central magnetic field B_0, consistently with Eq. (17). The pressure provided by the relativistic electrons is always smaller than the pressure of the thermal gas. Within R_h this holds in all cases also when the magnetic pressure is added to that of the electrons.
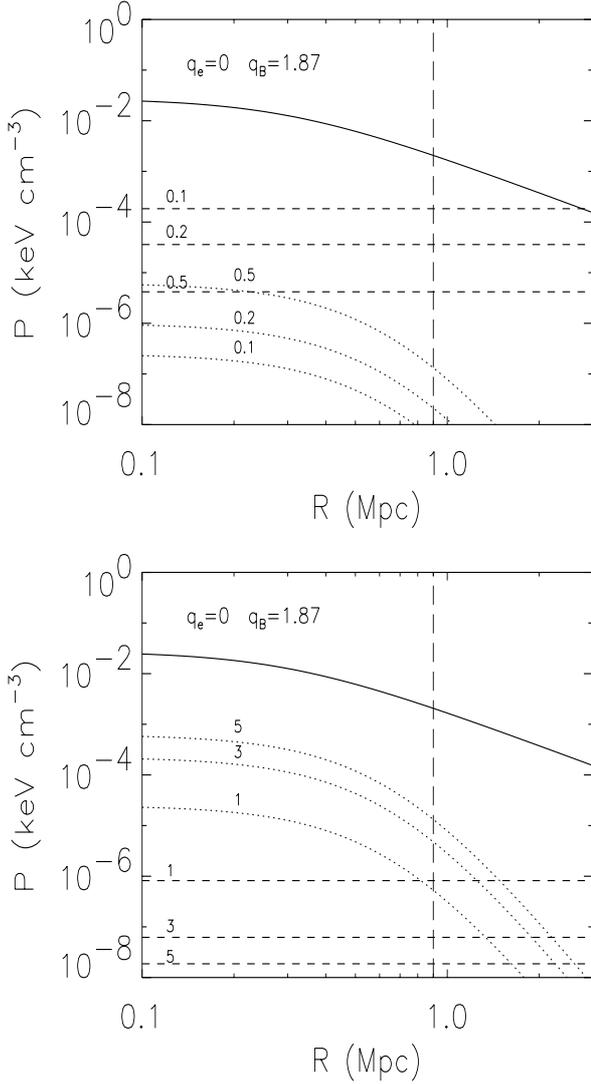
Fig. 3. The radial distribution of the pressure of the relativistic electrons (dashed) and the magnetic field (dotted) which fit the Coma radio-halo brightness. We show the predictions for models with $q_e = 0$ and $q_B = 1.87$ for values $B_0 = 0.1, 0.2$ and $0.5 \, \mu$G (*upper panel*) and for $B_0 = 1, 3$ and $5 \, \mu$G (*lower panel*). We also show the pressure of the thermal intra-cluster gas (solid) for comparison. The vertical dashed line is placed at $R_h = 0.9$ Mpc.

As emphasized in Sect. 3, the presence of scalar fluctuations in the magnetic field B would decrease the values of n_{rel}, given in Table 1, by the factor $[1 + \langle (\delta B)^2 \rangle / B^2]^{(\alpha_R + 1)/2}$.

5. Inverse Compton Scattering emission

In this section we use the radial profiles of the relativistic electrons and of the magnetic field, in any of the above mentioned combinations which fit the radio halo brightness distribution, to predict the brightness distribution of the HXR emission produced by ICS of the relativistic electrons on the CMB photons.

For the general case of a relativistic electrons distribution as in Eq. (1), it is imperative, in spherical symmetry, to introduce a maximum radius out to which it is assumed to hold, and beyond which it goes to zero. This is because the density
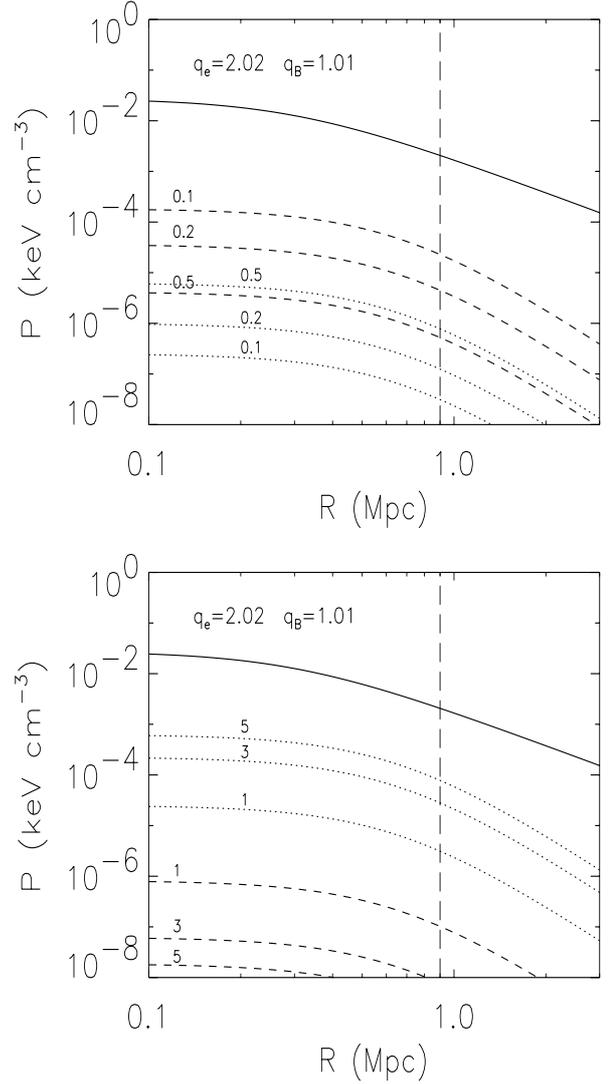
Fig. 4. Same as Fig. 3 but for models with $q_e = 2.02$ and $q_B = 1.01$.

of CMB photons is a constant, unlike the strength of the magnetic field, which is constrained, for any choice of q_e, by the radio brightness profile. Here we assume this radius equal to $R_{vir} = 3$ Mpc, corresponding to a maximum value of the angular distance from the centre $\Theta = 105$ arcmin.

Among the cases selected, it is evident from Figs. 3–5 that for some values of B_0, when either q_e or q_B are equal to zero, the non-thermal pressure does not always remain below the thermal one when one moves beyond R_h, and this need to be kept in mind. For simplicity we provide the ICS brightness predictions *in all cases* using the same value of Θ.

The HXR ICS surface brightness at the energy E_X and at the angular distance θ from the cluster center is

$$S_X(E_X, \theta) = S_{X,0} \left[1 + (\theta/\theta_{c,R})^2 \right]^{-q_e + 1/2} \qquad (18)$$
$$\cdot [\mathcal{B}(q_e - 1/2, 1/2) - \mathcal{B}_m(q_e - 1/2, 1/2)]$$

where $\mathcal{B}$ and $\mathcal{B}_m$ are the Beta and incomplete Beta functions, respectively (Abramowitz & Stegun 1972)

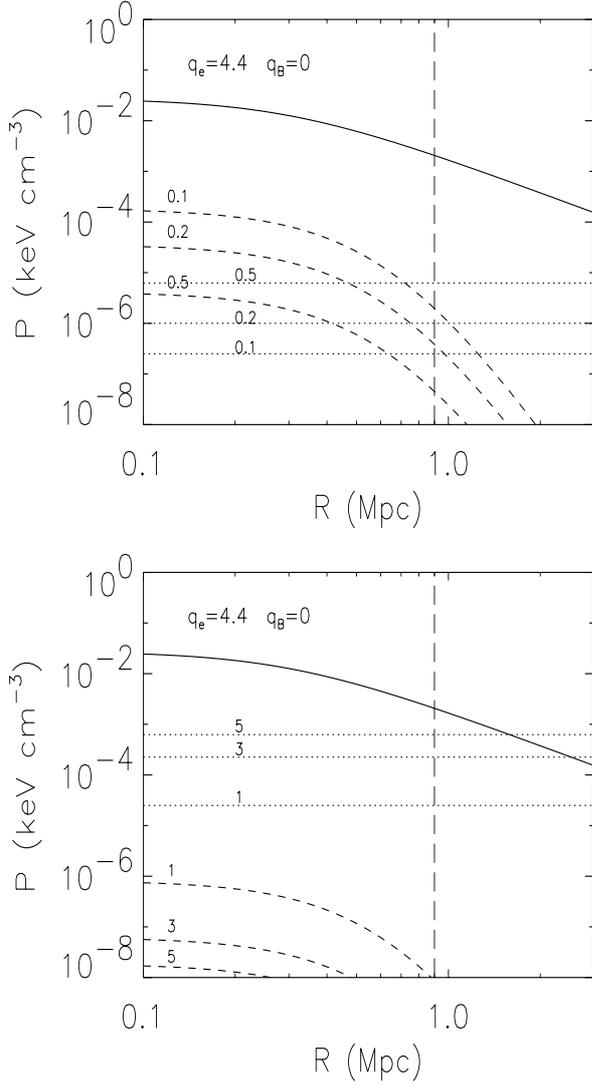$$\mathcal{B}(a, b) \equiv \int_0^1 t^{a-1} (1-t)^{b-1} dt \qquad (19)$$

Fig. 5. Same as Fig. 3 but for models with $q_e = 4.4$ and $q_B = 0$.

$$\mathcal{B}_m(a, b) \equiv \int_0^m t^{a-1}(1-t)^{b-1}\mathrm{d}t \tag{20}$$

with

$$m = \frac{1 + (\theta/\theta_{c,R})^2}{1 + (\Theta/\theta_{c,R})^2}. \tag{21}$$

Here

$$S_{X,0} = 4.17 \times 10^{-4} \times (8)^{\alpha_R - 1} \left(\frac{E_X}{\text{keV}}\right)^{-\alpha_R} \left(\frac{r_{c,R}}{\text{Mpc}}\right)$$

$$\cdot \left(\frac{n_{\text{rel},0}}{\text{cm}^{-3}\text{GeV}^{-1}}\right) \text{ erg s}^{-1} \text{ cm}^{-2} \text{ keV}^{-1} \text{ arcmin}^{-2}. \tag{22}$$

Specifically for Coma, the HXR surface brightness, in the 20–80 keV band, was calculated according to the choice of parameters described in Sects. 2 and 4, and reported in Table 1. Notice that $n_{\text{rel},0}$ depends only on the value of the central radio emissivity, while $\langle B \rangle$ represents the volume average out to $R_h = 0.9 \, h_{70}^{-1}$ Mpc. The brightness profiles, as a function of the angular distance from the center, are given in Figs. 6–11, which contain, for comparison, the brightness in the same spectral band of the thermal gas emission. It is evident that, within
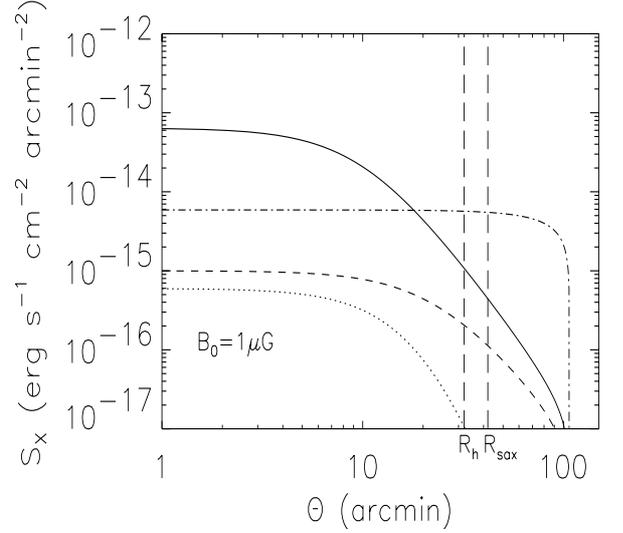

Fig. 6. The spatial distribution of the HXR brightness of the Coma cluster in the 20–80 keV energy band as produced by ICS of relativistic electrons reproducing the radio halo flux. We show the predictions for different models: $q_e = 0$ (dot-dashed curve), $q_e = 2.02$ (dashed curve) and $q_e = 4.4$ (dotted curve) for a value $B_0 = 1 \, \mu G$. The thermal bremsstrahlung brightness of Coma integrated in the same energy band (solid curve) is shown for comparison.
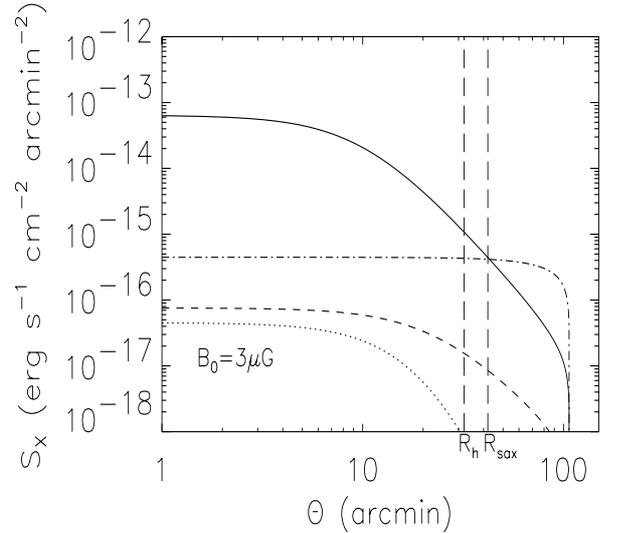

Fig. 7. Same as Fig. 6 but for $B_0 = 3 \, \mu G$.

$\Theta = 32'$ corresponding to R_h, the non-thermal HXR brightness, for appropriate values of q_e, can be comparable to, or greater than the thermal one only for values of B_0 less than $0.5 \, \mu G$. Beyond $\Theta = 32'$ the brightness is based upon extrapolations outside the maximum extent of the radio-halo, R_h, as measured so far. Spatially resolved HXR observation would shed light on the true distribution of the relativistic electrons (together with that of the magnetic field) not only within but also outside R_h. The necessary technical capabilities might be available with the upcoming dedicated experiments like, e.g., NeXT (e.g., Takahashi et al. 2004).

We conclude this section discussing how the volume averaged magnetic field strength should be computed when using
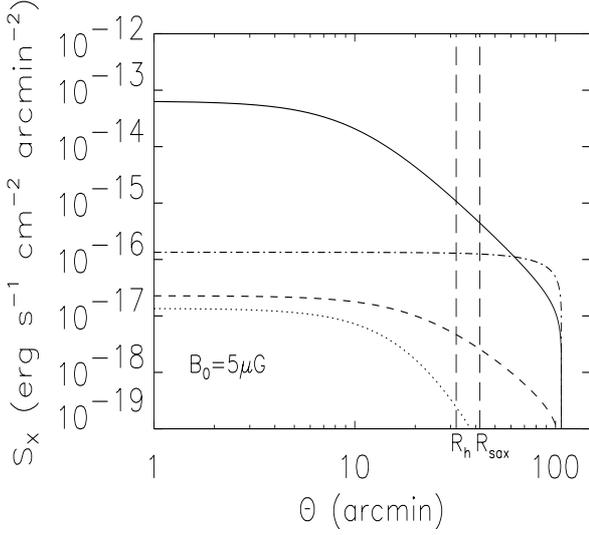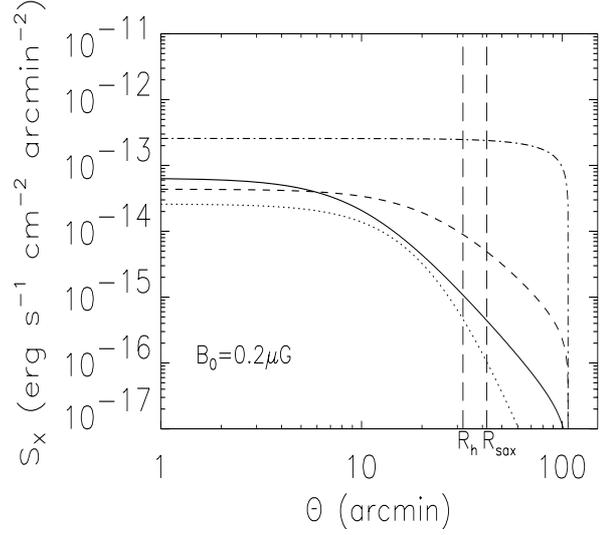
Fig. 8. Same as Fig. 6 but for $B_0 = 5\,\mu$G.

Fig. 10. Same as Fig. 6 but for $B_0 = 0.2\,\mu$G.

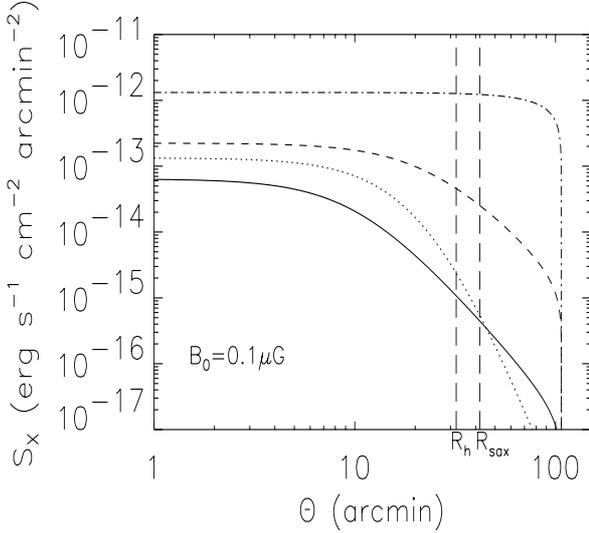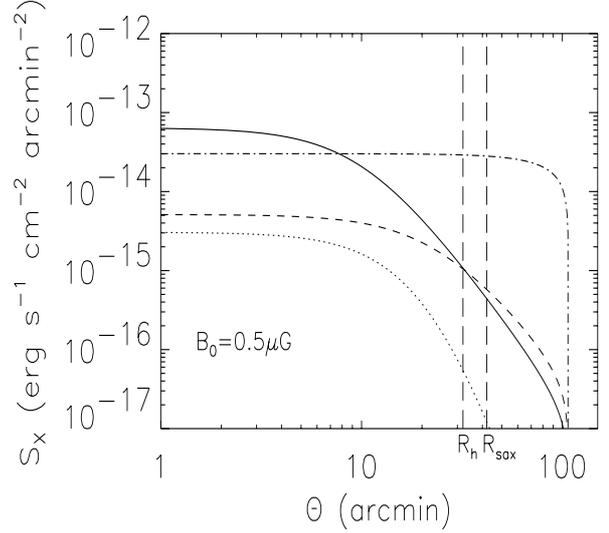**Fig. 9.** Same as Fig. 6 but for $B_0 = 0.1\,\mu$G.

Fig. 11. Same as Fig. 6 but for $B_0 = 0.5\,\mu$G.

integral values of the radio and the HXR (ICS) flux: cospatial radio and ICS flux values can be used to estimate the quantity $(B_{\mathrm{ICS}})^{\alpha_R+1} \propto F_{\mathrm{ICS}}/F_{\mathrm{radio}}$ (e.g. Carilli & Taylor 2002). In general, except for the case $B = $ constant, the inequality

$$\langle B^{\alpha_R+1}\rangle \neq \langle B\rangle^{\alpha_R+1}$$

holds, and the use of the right hand side of the inequality to estimate the average value of B (as in, e.g., Henriksen 1998; Fusco-Femiano et al. 1999, 2004) is formally incorrect, although quantitatively only by a modest factor. The value of this quantity differs from the actual value of $\langle B\rangle$ from Eq. (10) and depends on q_B, as it will be shown numerically in the next section.

6. Discussion

This Section will first address the conclusions on $\langle B\rangle$, that follow from available integral measurements. Then, it will

concentrate on the further constraints, that can be derived from FR measurements.

The integrated HXR flux from Coma has been measured with BeppoSAX and RossiXTE (Fusco-Femiano et al. 1999, 2004; Rephaeli et al. 1999). Both measurements found an excess on top of the thermal emission, with a flux of $F_{20-80} = (1.5 \pm 0.5) \times 10^{-11}$ erg s^{-1} cm^{-2} (Fusco-Femiano et al. 2004), and has been interpreted as ICS emission from the radio–halo. The BeppoSAX result is still controversial (see Rossetti & Molendi 2004), however, for the purpose of this discussion, it can, at worst, be regarded as an upper limit.

First we consider the case, discussed in Fusco-Femiano et al. (1999, 2004), that this flux is ICS from within the spherical volume of the radio-halo. Thus we use Eq. (18) with $\Theta = 32$ arcmin, corresponding to R_{h}, and the accordingly different normalization of Eq. (22). By equating the measured flux to the integral of S_X out to Θ, we obtain the results on B_0, $\langle B\rangle$ and $n_{\mathrm{rel},0}$ given in Table 2, for the three different combinations of q_{e} and q_{b}, used throughout this paper. The corresponding

Table 2. The parameters reported in this table are evaluated from the requirement that the ICS HXR emission from the radio-halo of Coma, assumed spherical, equals the flux observed by BeppoSAX. We report here the central value of the magnetic field B_0, the volume-averaged value $\langle B \rangle$ and the central density of the relativistic electrons $n_{\rm rel,0}$, for the three sets, used throughout this paper, of parameters on the relativistic electron and magnetic field distributions, which reproduce the Coma radio-halo brightness. The separate last line is the case where the electron distribution given in Fig. 2 is used.

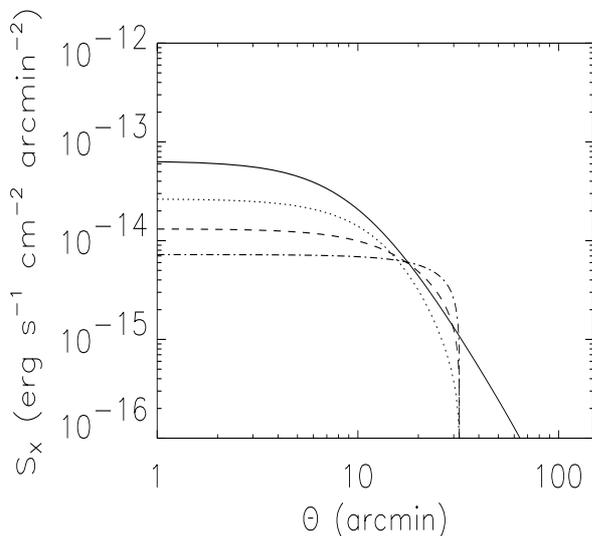| $q_{\rm e}$	$q_{\rm b}$	B_0 (μG)	$\langle B \rangle$ (μG)	$n_{\rm rel,0}$ (cm^{-3} GeV^{-1})
0	1.87	0.55	0.17	1.16×10^{-11}
2.02	1.01	0.32	0.16	4.20×10^{-11}
4.4	0	0.20	0.20	1.29×10^{-10}
–	–	1.10	0.18	2.37×10^{-12}

Fig. 12. The 20–80 keV brightness distributions in the Coma cluster, as produced by ICS of relativistic electrons within a sperical volume corresponding to the radio halo ($\Theta = 32$ arcmin): the normalizations are chosen to provide an integral value equal to the flux measured by Fusco-Femiano (2004). The three curves correspond to $q_{\rm e} = 0$ (dot-dashed), $q_{\rm e} = 2.02$ (dashed) and $q_{\rm e} = 4.4$ (dotted). The thermal bremsstrahlung brightness of Coma integrated in the same energy band (solid curve) is shown for comparison.

brightness profiles are shown in Fig. 12. As anticipated in the previous section, the three values of $\langle B \rangle$ are not identical, and we recover the one obtained by Fusco-Femiano et al. (2004), namely 0.2 μG, only if the magnetic field is constant, i.e. $q_B = 0$.

Within the two extremes for $q_{\rm e}$, 0 and 4.4, the central value B_0 decreases from 0.55 to 0.20 μG. The intermediate value, $B_0 = 0.32$ μG is probably the most "realistic", in that it corresponds to a radial decrease in both the relativistic electron density and in the magnetic field strength.

Referring to the considerations in Sect. 3 of the effects of scalar fluctuations in the magnetic field, this estimate should, in principle, be considered as an upper limit: by how much it

might differ from reality is hard to tell objectively but it could be evaluated by using specific models, a task beyond the goal of this paper.

On the other hand, some information on the strength of the field, along with the scale of its vectorial fluctuations, can and have been inferred from Faraday Rotation (FR) measurements, hence we now turn to their implications.

These measurements have been carried out in several Clusters (see, e.g., Clarke et al. 1999, 2001; Dolag et al. 2001, 2002) and various papers have been devoted to the uncertainties on the derivation of values for $B_\parallel$, which are related to the limited statistics on the number of independent measurements for the same cluster (Newman et al. 2002) or the approximations adopted for the spectrum of the fluctuations as a function of their scale-length (Enßlin & Vogt 2003; Murgia et al. 2004). When the FR measurements are made using embedded radio sources, the typical central field strength is found to be $\sim$10–30 μG (Eilek 1999), but in general terms FR measurements on background sources are considered more reliable. For Coma in particular, using data on background sources, Kim et al. (1991) found a value of $B_\parallel$ for the region within the X-ray core radius equal to 1.7 ± 0.9 μG. Furthermore, Feretti et al. (1995) found that fluctuations probably occur on all scales down to $\approx$1 kpc. For a random vectorial distribution, the previous estimate on $B_\parallel$ can be translated into an estimate of B_0 equal to 3.8 ± 2.0 μG.

Taken at face value, this quantity is significantly larger than B_0 given in Table 2, even in the most favourable assumption of $q_{\rm e} = 0$. Thus, the interpretation of the excess 20–80 keV flux, referred to above, in terms of ICS emission from the radio–halo, is hard to reconcile with these further constraints. The more so if the possible presence of scalar fluctuations, which would reduce B_0 below the strength given in Table 2, is not neglected.

One must however take into account that, for the time being, the excess HXR flux has been detected only with non-imaging instruments, thus it cannot be excluded that the ICS emission extends outside $R_{\rm h}$. The FWHM of the BeppoSAX PDS instrument used by Fusco-Femiano et al. (2004) covers the Coma Cluster out to an angular distance from the center $\theta = 42$ arcmin. If we integrate out to this radius the predicted ICS profiles, the ones given this time by Eqs. (18) and (22), we recover the excess HXR flux for values of $B_0 = 1.37, 0.40, 0.20$ μG for $q_{\rm e} = 0, 2.02$ and 4.4 respectively. However, even if we do so, we come close to the central B value estimated through the FR measurements only with $q_{\rm e} = 0$, a rather unlikely hypothesis, although, as can be judged from Fig. 3, the non-thermal pressure remains well below the thermal one out to $R_{\rm vir}$, and therefore cannot be discarded on these grounds.

If one accepts this hypothesis, it follows that most of the HXR emission should be produced by relativistic electrons located in the outer regions of the cluster. Conversely, the radio-halo emission is dominated by relativistic electrons located in the central part of Coma and certainly at distances smaller than $R_{\rm h}$. The electrons that produce the bulk of the HXR emission are thus different from those producing the bulk of the radio-halo emission. This is a consequence of the assumption
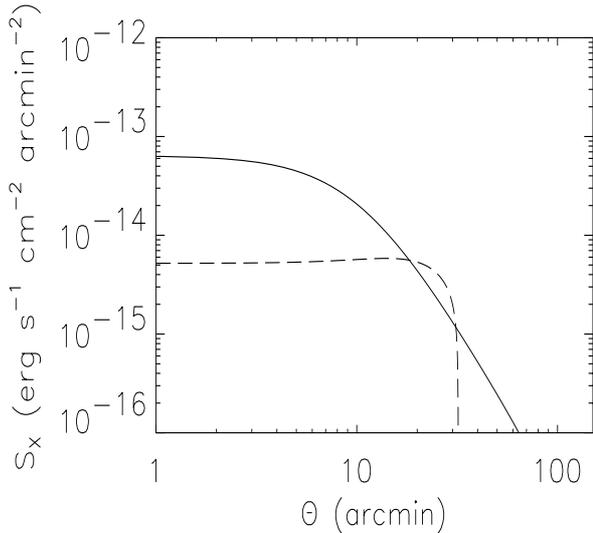
Fig. 13. Same as Fig. 12, for the relativistic electron distribution given in Fig. 2.

of an extended, diffuse HXR emission originating from ICS of CMB photons off relativistic electrons. We note here that the different spatial location of the radio-halo emission and of the bulk of the HXR emission is also a prediction of various models invoked to reproduce the formation of the Coma radio-halo (see, e.g., Brunetti et al. 2001; Kuo et al. 2003).

Finally we have considered also the relativistic electron distribution illustrated in Fig. 2, which follows from assuming $B(r)$ proportional to $n_{th}(r)$, as from hydrodynamical simulations (Dolag et al. 2002). The HXR brightness profile is shown in Fig. 13. Most of the electrons are confined in the outer regions of the radio-halo, with a density peaking at about $0.8R_h$, and it turns out (upon integration over a spherical volume with radius R_h, last and separate line in Table 2) that $B_0 = 1.1\ \mu G$, two times larger than for $q_e = 0$, and much closer to the estimate from FR measurements. Thus, the same comment applied to the previous hypothesis remains valid, namely that most of the electrons responsible for the ICS emission are other than those responsible for most of the radio emission, although both are fully confined within R_h.

These considerations make it very clear that to properly address this issue we badly need spatially resolved observations in the HXR band, where new generation telescopes are being designed to operate. Obviously the success will depend more on sensitivity and particle background than on angular resolution, which could be in the order of one arcmin for this special purpose.

To conclude the discussion, we remark that the EUV emission excess found in the Coma cluster in the energy band 65–200 eV (see, e.g., Lieu et al. 1996; Bowyer et al. 1999, 2004) does not have any implication for our results. In fact, relativistic electrons which emit in the mentioned EUV band by ICS, emit by synchrotron radiation in the frequency range $\nu \sim (0.13-0.4)\ B_\mu$ MHz. Thus, these electrons should emit synchrotron radiation in the observed radio band ($\nu \geq 30$ MHz) only for a magnetic field $B \geq 75\ \mu G$, a situation that can be excluded on several grounds, the most obvious being that the magnetic pressure would largely exceed the thermal pressure.

This is not to exclude that the EUV emission excess might itself be due to IC emission, as proposed for instance by Bowyer et al. (2004). This is another, open problem, to which we devote an independent paper (Marchegiani et al., in preparation).

7. Summary and conclusions

Radio halos, that is diffuse synchrotron emission in clusters of galaxies, is a rather common phenomenon that implies the presence of a non-thermal intracluster component, in addition to the thermal component that gives rise to the diffuse X-ray emission. Unlike the latter, whose density and temperature distributions can be directly inferred from X-ray measurements, the former is a combination of relativistic electrons and magnetic fields, whose relative weight in the radio emissivity cannot be deduced on the basis of the observed radio properties alone. In order to resolve the degeneracy between these two parameters, an independent estimate of either one or the other is required.

For the relativistic electrons this estimate can be obtained by measuring their unavoidable emission through Inverse Compton Scattering on the photons of the Cosmic Microwave Background. For astrophysically reasonable values of the magnetic field, the ICS emission by the same electrons responsible for the radio emission should fall in the HXR, roughly in the range 10–100 keV, and could therefore be easily separated, given adequate sensitivity in that range, from the thermal emission on spectral grounds.

Alternatively, Faraday Rotation measurements on background radio sources, seen through the cluster, can provide an absolute estimate of the magnetic field, given the available constraints on the contribution to the rotation by the thermal electrons.

This paper, using the radio-halo in Coma as a case-study and its brightness radial distribution as the only constraint, concentrates on predicting the HXR (20–80 keV) brightness distribution of the ICS emission, for different, model-independent, central values and radial behaviours of the magnetic field (or, equivalently, of the density of the relativistic electrons). Such predictions could be valuable to establish requirements on sensitivity for the next generation of hard X-ray imaging telescopes. Spatially resolved observations would tell us directly the density distribution of the relativistic electrons, and consequently of the B field. We wish to stress that such measurements would give us information not only on the smooth radial dependence of B, but also of its scalar fluctuations on small scales. These fluctuations, because of the non-linear dependence of the radio emissivity on the field strength, imply systematically a smaller number of electrons for the same radio flux, and consequently they reduce the HXR brightness for the same value of the locally averaged value of B.

The Coma Cluster is a case where detection of a HXR tail on top of the thermal emission has already been claimed (Fusco-Femiano et al. 2004; Rephaeli et al. 1999). We use the value of this excess flux to estimate the central value of the field, B_0, for three different forms of the radial distribution of its smooth component, and a random, isotropic distribution of its direction on scales much smaller than the size of the radio-halo. We do this either assuming that the electrons and

magnetic fields are completely confined within the borders of the radio-halo, as determined so far, or assuming that the distributions adopted in our predictions extend out to the virial radius, R_{vir}, of Coma. In the first case we find values of B_0 between 0.2 and 0.55 μG, with the largest value corresponding to an electron density constant with radius (the volume averaged value of B is exactly equal to the value of 0.2 μG obtained by Fusco-Femiano et al. (2004) only if B is assumed constant). In the second case, taking into account the field of view of the instrument used by Fusco-Femiano et al. (2004), we find values between 0.2 and 1.4 μG. Again, the largest value obtains if the relativistic electron density is assumed constant with radius, a rather unlikely possibility, which however we cannot exclude simply on dynamical grounds, because their pressure remains below that of the thermal gas extrapolated out to R_{vir}. The intermediate form of the radial distribution of B yields $B_0 = 0.4 \, \mu$G.

As a third case, we consider the possibility, supported by hydrodynamical simulations (Dolag et al. 2002), that $B(r)$ is proportional to $n_{th}(r)$. This implies a rather peculiar relativistic electron density distribution, which has its minimum value at the center and peaks at about $0.8R_h$. Upon integration over the spherical volume within R_h, the HXR flux measured by Fusco-Femiano et al. (2004) is recovered with $B_0 = 1.1 \, \mu$G.

A comparison with estimates from FR measurements is then made. Although such estimates are still controversial, a value of B_0 equal to 1–2 μG seems likely. Consistency with the estimates from the HXR excess is at best marginal. The more so if one considers that the latter were obtained ignoring the (admittedly hard to quantify in a model-independent way) scalar fluctuations, whose presence would decrease the value of B_0. Moreover, if the claimed HXR excess emission is really there, and it is due to ICS, it would follow that the electrons responsible for the bulk of this emission are mostly distributed outside the region where the electrons responsible for the bulk of the radio emission reside. It is then evident that measurements of the HXR brightness distribution, whose prediction is the main goal of this paper, are a necessary step to clarify this important issue.

References

Abramowitz, A., & Stegun, I. A. 1972, Handbook of Mathematical Functions (New York: Dover)

Bowyer, S., Berghofer, T. W., & Korpela, E. J. 1999, ApJ, 526, 592

Bowyer, S., Korpela, E. J., Lampton, M., & Jones, T. W. 2004, ApJ, 605, 168

Brunetti, G., Setti, G., Feretti, L., & Giovannini, G. 2001, MNRAS, 320, 365

Brunetti, G. 2003, in Matter and Energy in Clusters of Galaxies, ed. S. Bowyer, & C.-Y. Hwang, ASP Conf. Ser., 301, 349

Carilli, C. L., & Taylor, G. B. 2002, ARA&A, 40, 319

Clarke, T. E., Kronberg, P. P., & Bohringer, H. 1999, in Diffuse Thermal and Relativistic Plasma in Galaxy Clusters, ed. H. Bohringer, L. Feretti, & P. Schuecker, MPE Rep., 271, 82

Clarke, T. E., Kronberg, P. P., & Bohringer, H. 2001, ApJ, 547, L111

Deiss, B., Reich, W., Lesch, H., & Wielebinski, R. 1997, A&A, 321, 55

Dolag, K., Schindler, S., Govoni, F., & Feretti, L. 2001, A&A, 378, 777

Dolag, K., Bartelmann, M., & Lesch, H. 2002, A&A, 387, 383

Eilek, J. 1999, in Diffuse Thermal and Relativistic Plasma in Galaxy Clusters, ed. H. Bohringer, L. Feretti, & P. Schuecker., MPE Rep., 271, 71

Enßlin, T. A., & Vogt, C. 2003, A&A, 401, 835

Feretti, L. 2003, in Matter and Energy in Clusters of Galaxies, ed. S. Bowyer, & C.-Y. Hwang, ASP Conf. Ser., 301, 143

Feretti, L., Dallacasa, D., Giovannini, G., & Tagliani, A. 1995, A&A, 302, 680

Fusco-Femiano, R., Dal Fiume, D., Feretti, L., et al. 1999, ApJ, 513, L21

Fusco-Femiano, R., Orlandini, M., Brunetti, G., et al. 2004, ApJ, 602, L73

Giovannini, G., Feretti, L., Venturi, T., et al. 1993, ApJ, 406, 399

Gonçalves, D. R., & Friaça, A. C. S. 1999, MNRAS, 309, 651

Harris, D. E., & Grindlay, J. E. 1979, MNRAS, 188, 25

Henriksen, M. 1998, PASJ, 50, 389

Kempner, J. C., & Sarazin, C. L. 2001, ApJ, 548, 639

Kim, K. T., Kronberg, P. P., & Tribble, P. C. 1991, ApJ, 379, 80

Kuo, P.-H., Huang, C.-Y., & Ip, W.-H. 2003, ApJ, 594, 732

Lieu, R., Mittaz, J. P. D., Bowyer, S., et al. 1996, Science, 274, 1335

Lokas, E. L., & Mamon, G. A. 2003, MNRAS, 343, 401

Longair, M. 1994, High Energy Astrophysics, vol. 2 (Cambridge University Press)

Murgia, M., Govoni, F., Feretti, L., et al. 2004, A&A, 424, 429

Newman, W. I., Newman, A. L., & Rephaeli, Y. 2002, ApJ, 575, 755

Perola, G. C., & Reinhardt, M. 1972, A&A, 17, 432

Rephaeli, Y. 1979, ApJ, 227, 364

Rephaeli, Y., Gruber, D., & Blanco, P. 1999, ApJ, 511, L21

Rossetti, M., & Molendi, S. 2004, A&A, 414, L41

Takahashi, T., Makishima, K., Fukazawa, Y., et al. 2004, New AR, 48, 269

Thierbach, M., Klein, U., & Wielebinski, R. 2003, A&A, 397, 53